https://doi.org/10.31436/iiumej.v26i3.3634

PROPOSED CONVBILSTM-NET MODEL FOR ENHANCING EARTHQUAKE PREDICTION PERFORMANCE USING SPATIOTEMPORAL FEATURES

ARI FADLI[1,3], TRI KUNTORO PRIAMBODO[1*], AGFIANTO EKO PUTRA[1], WIWIT SURYANTO[2]

[1]*Department of Computer Science and Electronics, Universitas Gadjah Mada, Yogyakarta, Indonesia*
[2]*Department of Physics, Universitas Gadjah Mada, Yogyakarta, Indonesia*
[3]*Electrical Engineering, Universitas Jenderal Soedirman, Purwokerto, Indonesia*

**Corresponding author: mastri@ugm.ac.id*

(Received: 3 March 2025; Accepted: 15 July 2025; Published online: 9 September 2025)

ABSTRACT: Accurate earthquake prediction remains a significant challenge due to the complex spatiotemporal dependencies inherent in seismic events. To address this issue, the present study proposes ConvBiLSTM-Net. This hybrid deep learning model combines Convolutional Neural Networks (CNNs) for spatial feature extraction with Bidirectional Long Short-Term Memory (BiLSTM) networks for temporal sequence modeling. The model integrates historical earthquake data with spatial information in the form of fault density (FD), derived using Kernel Density Estimation (KDE). The KDE bandwidth is optimized using the Bivariate Local Indicator of Spatial Association (LISA) method to enhance spatial adaptivity. The dataset comprises earthquake records from the USGS catalog (1974–2023) and active fault data compiled in the 2017 Indonesian Earthquake Source and Hazard Map, published by the National Earthquake Study Center (PuSGeN). ConvBiLSTM-Net is evaluated under short-term and medium-term prediction scenarios, targeting earthquake magnitude, depth, and epicenter coordinates (latitude and longitude), using standard performance metrics such as accuracy, F1 score, root mean square error (RMSE), mean absolute error (MAE), and the coefficient of determination (R^2). In the short-term scenario, the model achieves average improvements of 9.31% in R^2, 3.41% in accuracy, and 6.06% in F1 score, while reducing RMSE by 10.63% and MAE by 12.40% across magnitude, depth, and latitude predictions. For longitude, R^2, accuracy, and F1 score also improve by 10.88%, 11.76%, and 17.54%, respectively, although RMSE and MAE increase by 13.09% and 20.74%, indicating a trade-off between enhanced pattern recognition and higher absolute error. Under the medium-term scenario, the model demonstrates average improvements of 7.49% in R^2, 3.39% in accuracy, and 7.06% in F1 score, while reducing RMSE and MAE by 6.22% and 17.72%, respectively, for magnitude, depth, and latitude predictions. For longitude, R^2, accuracy, and F1 score improve by 12.50%, 2.48%, and 1.60%, respectively, though RMSE and MAE increase by 37.31% and 37.01%, again highlighting a trade-off between better pattern recognition and increased absolute error in this dimension. These findings demonstrate that ConvBiLSTM-Net, engineered to integrate spatial and temporal features, is a robust and adaptive architecture for enhancing earthquake prediction performance. Its spatiotemporal modeling approach yields consistently high accuracy and stability across forecasting horizons, particularly in predicting earthquake epicenters. Despite minor trade-offs in absolute error for longitude predictions, the overall performance improvements affirm its potential as a reliable tool for seismic hazard assessment and disaster risk mitigation.

ABSTRAK: Ramalan gempa bumi yang tepat kekal sebagai satu cabaran utama disebabkan oleh kebergantungan spatiotemporal yang kompleks dalam kejadian seismik. Bagi menangani isu ini, kajian ini mencadangkan ConvBiLSTM-Net, iaitu sebuah model hibrid pembelajaran mendalam yang menggabungkan Rangkaian Neural Konvolusional (CNN) dan Memori

Jangka Pendek Dwi Arah (BiLSTM), bagi tujuan pengekstrakan ciri spatial dan pemodelan jujukan temporal, masing-masing. Model ini menggabungkan data sejarah gempa bumi dengan maklumat spatial dalam bentuk ketumpatan sesar (fault density, FD), yang diperoleh melalui Kaedah Anggaran Ketumpatan Kernel (Kernel Density Estimation, KDE). Lebar jalur KDE dioptimumkan menggunakan kaedah Bivariate Local Indicator of Spatial Association (LISA) bagi meningkatkan kepekaan spatial. Set data kajian merangkumi rekod gempa bumi daripada katalog USGS (1974–2023) serta data sesar aktif yang disusun dalam Peta Sumber dan Bahaya Gempa Indonesia 2017, terbitan Pusat Kajian Gempa Nasional (PuSGeN). Model ConvBiLSTM-Net ini dinilai dalam dua senario ramalan—jangka pendek dan jangka sederhana—bagi parameter magnitud, kedalaman, serta koordinat pusat gempa (latitud dan longitud), dengan menggunakan metrik standard seperti ketepatan, skor F1, RMSE, MAE dan pekali penentuan (R^2). Malalui senario jangka pendek, model mencatatkan purata peningkatan sebanyak 9.31% pada R^2, 3.41% pada ketepatan, dan 6.06% pada skor F1; serta pengurangan RMSE sebanyak 10.63% dan MAE sebanyak 12.40% merentas ramalan magnitud, kedalaman, dan latitud. Bagi dimensi longitud, R^2, ketepatan, dan skor F1 turut meningkat sebanyak 10.88%, 11.76%, dan 17.54% masing-masing; namun begitu, RMSE dan MAE meningkat sebanyak 13.09% dan 20.74%, menunjukkan kompromi antara pengecaman corak yang lebih baik dan ralat mutlak yang lebih tinggi. Manakala senario jangka sederhana, model mencatatkan purata peningkatan sebanyak 7.49% pada R^2, 3.39% pada ketepatan, dan 7.06% pada skor F1; serta pengurangan RMSE sebanyak 6.22% dan MAE sebanyak 17.72% merentas tugas ramalan magnitud, kedalaman, dan latitud. Bagi dimensi longitud, peningkatan masing-masing dicatatkan pada R^2 (12.50%), ketepatan (2.48%), dan skor F1 (1.60%), tetapi RMSE dan MAE meningkat secara ketara sebanyak 37.31% dan 37.01%, menunjukkan kompromi antara pengecaman corak yang lebih kukuh dan ralat mutlak yang lebih besar pada dimensi ini. Dapatan kajian ini membuktikan bahawa ConvBiLSTM-Net, yang direka bentuk bagi menggabungkan ciri-ciri spatial dan temporal, merupakan satu seni bina model yang teguh dan adaptif dalam meningkatkan prestasi ramalan gempa bumi. Pemodelan spatiotemporal bersepadu yang digunakan menghasilkan tahap ketepatan dan kestabilan yang tinggi secara konsisten merentasi pelbagai ufuk ramalan, terutamanya dalam menentukan lokasi pusat gempa bumi. Walaupun terdapat sedikit kekurangan dalam nilai ralat mutlak bagi ramalan longitud, peningkatan prestasi secara keseluruhan mengesahkan nilainya sebagai alat yang boleh dipercayai dalam penilaian bahaya seismik dan pengurangan risiko bencana.

KEYWORDS: *Deep learning, earthquake prediction, kernel density estimation (KDE), spatial–temporal features.*

1. INTRODUCTION

Earthquakes are among the most destructive natural disasters, occurring without warning and resulting in significant human and economic losses [1]. They can trigger secondary hazards such as fires, infrastructure collapse, and tsunamis, further exacerbating their impact on lives and property. Since 1998, more than 750,000 people have died due to earthquakes, primarily in seismically active countries such as Japan, China, and Indonesia [2]. Based on their causes, earthquakes are generally categorized into three types: tectonic earthquakes (caused by plate movements), volcanic earthquakes (resulting from volcanic activity), and impact earthquakes (caused by collisions with extraterrestrial objects such as meteorites) [3]. Several significant events have resulted in catastrophic damage, including the 2011 Tōhoku earthquake in Japan (magnitude 9.1, approximately 20,000 deaths, and $360 billion in losses), the 2015 Nepal earthquake (magnitude 7.8, 8,964 deaths, and $10 billion in losses), and the 2023 Turkey–Syria earthquake (magnitude 7.5, 45,000 deaths, and $100 billion in losses) [4]. These disasters underscore the critical need for global cooperation in disaster preparedness, response, and recovery to mitigate future risks.

Earthquake prediction is typically classified into three categories based on temporal scale: long-term prediction (ranging from hundreds to thousands of years), medium-term prediction (spanning decades to a few years), and short-term prediction (ranging from a few days to one week) [5-7]. This classification has served as a conceptual framework for developing predictive methodologies across various disciplines, including mathematics, statistics, and artificial intelligence (AI) [8]. While statistical and mathematical models have shown consistent utility in earthquake forecasting [9,10], their limitations in capturing seismic phenomena‘ highly nonlinear and spatiotemporal nature remain evident.

Recent advances in AI, particularly in machine learning (ML) and deep learning (DL), have introduced a paradigm shift in predictive seismology. These data-driven approaches excel in extracting latent patterns from complex, high-dimensional seismic datasets without relying on handcrafted features. A comprehensive meta-analysis of 84 scientific publications highlights that AI-based methods outperform traditional prediction accuracy and adaptability models, ranging from rule-based fuzzy inference systems to modern deep neural networks. Furthermore, these approaches offer scalable, region-specific solutions for real-time earthquake forecasting. This growing body of evidence reinforces the transformative role of AI in bridging critical gaps in seismic risk assessment and early warning systems, particularly for short-term prediction scenarios [11].

Consequently, AI-based techniques are increasingly recognized as indispensable tools for enhancing modern earthquake prediction systems’ accuracy, responsiveness, and reliability. The broader success of AI, including ML and DL, in predictive analytics further underscores their relevance. Enabled by rapid advancements in computational power, these methods have demonstrated exceptional capabilities in identifying complex patterns within large-scale datasets, making them particularly effective for addressing nonlinear and dynamic forecasting challenges. Their influence is especially notable in information science and technology, where they have been successfully applied across various domains [12-14].

For example, Huang et al. [15] employed an ensemble approach for wind speed prediction; Peng et al. [16] combined Random Forest with Long Short-Term Memory (LSTM) networks to forecast tourist arrivals; Li and Wu [17] utilized clustering techniques for market style prediction; and Wang et al. [18] applied ensemble methods to model customer churn. Moreover, AI- and DL-based approaches have demonstrated strong capabilities in anomaly detection, further validating their applicability across diverse predictive modeling tasks. These cross-domain applications highlight the potential of AI-driven frameworks to address the complex spatiotemporal characteristics inherent in earthquake prediction.

ML and DL methodologies have been extensively adopted in earthquake prediction research, commonly formulated as classification or regression problems. Classification-based approaches typically frame earthquake prediction as a binary decision task, determining whether an earthquake exceeding a predefined magnitude threshold will likely occur within a specific time window. For instance, Asim et al. employed various ML classifiers to predict the occurrence of earthquakes with magnitudes ≥ 5.5 in the Hindukush region within a one-month forecasting window, utilizing seismic indicators derived from historical earthquake catalogs [19]. In a subsequent study, Asim et al. [20] implemented Support Vector Regression (SVR) and Hybrid Neural Networks (HNN), optimized via Enhanced Particle Swarm Optimization (EPSO), to predict earthquakes with magnitudes greater than 5.0 in regions including the Hindu Kush, Chile, and Southern California. Similarly, Yaghmaei-Sabegh and Tsang [21] developed an Artificial Neural Network (ANN)-based site classification model using horizontal-to-vertical spectral ratio curves. Additional studies have integrated seismicity analysis with ML

algorithms, such as Support Vector Machines (SVM), Random Forest (RF), and ANN, to forecast earthquake occurrences in regions like Cyprus [22].

Regression-based models, in contrast, aim to predict specific earthquake parameters such as magnitude, timing, and location. Jain et al. developed predictive models leveraging location and depth features from United States Geological Survey (USGS) data, applying a range of ML algorithms including RF, Multi-Layer Perceptron (MLP), and SVR. Their findings revealed that the MLP model achieved the lowest root mean square error (RMSE) among all tested models, indicating superior performance in earthquake location prediction [23]. Similarly, Gonzalez et al. proposed using Recurrent Neural Networks (RNNs), specifically Gated Recurrent Units (GRUs), to model the spatiotemporal dynamics of seismic activity in Italy. Their model was trained on seismic data from 1995 to 2018 and could estimate the location, timing, magnitude, and depth of earthquakes moments before they occurred [24]. These findings highlight the efficacy of regression-based approaches, particularly deep learning architectures such as MLP and GRU, in capturing complex spatial and temporal relationships essential for accurate earthquake parameter prediction.

DL techniques have substantially improved earthquake forecasting because they can model intricate temporal dependencies using deep neural architectures. These models, which consist of multiple hidden layers and interconnected neurons, demonstrate enhanced generalization capabilities compared to shallow networks [25]. Wang et al. applied Long Short-Term Memory (LSTM) networks to capture spatiotemporal correlations among earthquake events across various regions in China. Their model included a dropout layer to mitigate overfitting, employed the Softmax function for activation, and was optimized using the RMSprop algorithm. The approach yielded superior predictive performance relative to traditional techniques [8]. Similarly, Cai et al. [26] proposed an LSTM-based prediction model for automated anomaly detection in earthquake precursor data, drawing on multi-disciplinary datasets. Their results indicated that LSTM networks effectively captured temporal patterns in normal behavior across diverse precursor sources, without requiring extensive domain-specific preprocessing. These outcomes suggest that LSTM networks possess strong potential for modeling complex temporal dynamics in seismic forecasting.

Fabregas et al. developed a system that integrates a Rule-Based Algorithm with LSTM networks to estimate earthquake frequency, maximum magnitude, and average depth over one year [27]. Berhich et al. [28] proposed a location-aware earthquake prediction approach using recurrent neural networks, including LSTM, Gated Recurrent Units (GRU), and their hybrid configurations. They applied K-Means clustering based on geographic features to segment seismic data from Morocco, Japan, and Turkey, effectively capturing region-specific seismic patterns. The results demonstrated strong predictive performance, particularly for high-magnitude events, with improved mean absolute error (MAE), mean squared error (MSE), and root mean squared error (RMSE) compared to previous studies.

Kail et al. [29] introduced a hybrid neural network combining Convolutional Neural Networks (CNNs) for spatial feature extraction with LSTM networks for temporal modeling. This integrated architecture significantly enhanced mid-term earthquake prediction performance, reducing false alarms by approximately 81% while maintaining comparable sensitivity in detecting actual events. Similarly, Bhandarkar et al. [30] empirically demonstrated that LSTM models significantly outperform feedforward neural networks (FFNN) in modeling earthquake trends, achieving a 59% improvement in the coefficient of determination (R^2).

Collectively, these studies highlight the effectiveness of hybrid and recurrent deep learning models in earthquake prediction. By integrating CNNs for spatial feature extraction with LSTM or GRU networks for temporal sequence modeling, these approaches have achieved notable improvements in predictive accuracy, including reduced error rates, enhanced sensitivity to region-specific seismic characteristics, and substantially lower false alarm rates, thereby offering a robust framework for reliable seismic forecasting.

Recent research has further advanced hybrid deep learning models to improve the accuracy and generalizability of earthquake prediction. Kavianpour et al. [31] developed a hybrid model incorporating Attention Mechanisms, CNN, BiLSTM, and Zero-Order Hold (ZOH) preprocessing to forecast earthquake magnitude and frequency across seismic regions in China. This model achieved superior performance, with an RMSE of 0.074, MAE of 0.076, and an R^2 of 0.906. In a related study, Kavianpour et al. [32] designed a CNN–BiLSTM model to predict monthly mean earthquake magnitudes in Japan. Building upon this foundation, the present study introduces an enhanced architecture, HC_BiLSTM, with several refinements to improve predictive accuracy. The model achieved the lowest RMSEs of 0.1170 and 0.0982 across two study areas.

Geng et al. [33] proposed deep temporal convolutional networks (DCTCNN and CNN-LSTM) to address long-term dependencies in seismic time series data. Their models outperformed traditional methods such as ARIMA, Support Vector Regression (SVR), Random Forest (RF), and baseline deep learning approaches. Specifically, DCTCNN achieved an RMSE of 0.0061 and an MAE of 0.070, corresponding to over 96.9% improvement in RMSE and 55.97% in MAE.

These recent advancements underscore the effectiveness of hybrid deep learning architectures in earthquake prediction. Models that combine convolutional layers (e.g., CNN or Temporal Convolutional Networks [TCN]) for spatial feature extraction with recurrent layers (e.g., LSTM or BiLSTM) to capture temporal dependencies, often enhanced by Attention Mechanisms or ZOH preprocessing, consistently outperform both traditional statistical methods and standalone deep learning models.

Despite recent advances, most studies have focused exclusively on temporal patterns, without explicitly incorporating spatial information into the modeling process [34]. However, empirical evidence indicates that destructive earthquakes predominantly occur near active fault zones [35-37], highlighting the importance of spatial features such as Fault Density (FD). FD represents the level of tectonic fragmentation in the Earth's crust and can be estimated using the spatial distribution of earthquake events around fault lines [34,38].

To address this research gap, the present study proposes a novel hybrid deep learning model called ConvBiLSTM-Net, which integrates spatial and temporal dependencies. The architecture combines Convolutional Neural Networks (CNNs) for spatial feature extraction with Bidirectional Long Short-Term Memory (BiLSTM) networks for temporal sequence modeling. Spatial features include fault density (FD), computed via kernel density estimation (KDE), with bandwidth optimized using a bivariate Local Indicator of Spatial Association (LISA), in contrast to previous studies that employed Bivariate Moran's Index for bandwidth selection [34,38]. This study adopts bivariate LISA to capture localized spatial autocorrelation in fault distribution better, as it enables the detection of spatial clusters and outliers that may be masked by global measures such as Bivariate Moran's Index [39]. Temporal features are derived from historical earthquake sequences. The remainder of this paper is structured as follows: Section 2 outlines the methodology, Section 3 presents the results and discussion, and Section 4 concludes the study.

https://doi.org/10.31436/iiumej.v26i3.3634

2. METHODOLOGY

This section outlines the methodology for developing the proposed earthquake prediction model based on deep learning. The model was implemented in Python 3.9, utilizing TensorFlow 2.15 (Keras API) for deep learning, scikit-learn 1.4 for data preprocessing, GeoPandas 0.14 for spatial data manipulation, and GDAL 3.8 for raster data processing. All experiments were conducted on a local computing environment equipped with an NVIDIA GeForce RTX 3050 Laptop GPU and 16 GB of RAM. This provided adequate computational efficiency and ensured reproducibility throughout the study. The model is designed to predict earthquake magnitude, depth, and location. A comprehensive earthquake catalog was employed to enhance the accuracy and reliability of the prediction outcomes.

2.1. Architecture of the ConvBiLSTM-Net Model

The deep learning model developed in this study to predict earthquake magnitude, depth, and epicentral location is termed ConvBiLSTM-Net. The overall architecture of the model is illustrated in Fig. 1. It integrates Convolutional Neural Networks (CNNs) for spatial feature extraction, Bidirectional Long Short-Term Memory (BiLSTM) layers for temporal sequence learning, and fully connected Dense layers for final prediction. This hybrid architecture is designed to effectively capture the complex spatiotemporal dependencies inherent in earthquake catalog data.

The network begins with an input layer that receives feature vectors comprising both temporal indicators (e.g., statistical seismic features) and spatial attributes (e.g., fault density). These inputs are processed through a convolutional block consisting of a convolutional layer, a batch normalization layer, and a max pooling layer.

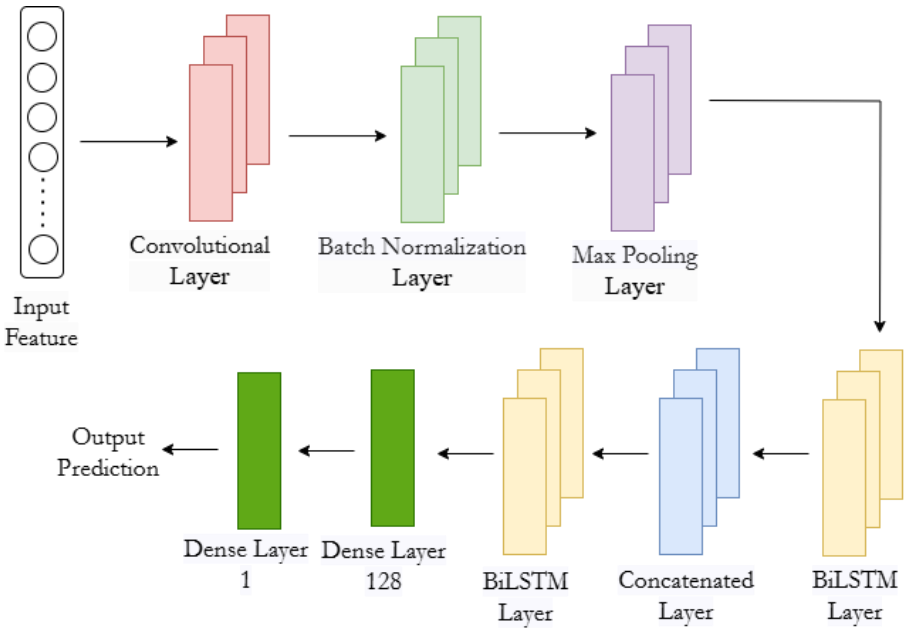

Figure 1. The structure of the ConvBiLSTM-Net

The convolutional layer applies multiple filters to extract local feature patterns. The output at position (i, j) in the l^{th} layer is computed as in Equation (1) [32].

$$y_{i,j}^{l} = ReLU\left(b_j^l + \sum_{m=1}^{M} w_{m,j}^{l} * x_{i+m-1,j}\right) \quad (1)$$

Here, * denotes a 1D convolution operation, b_j^l is the bias term, ω represents the filter weights, and m indexes the kernel position. The activation function used is ReLU, defined as $RELU\ (x) = \max(0, x)$, which enables efficient convergence and mitigates the vanishing gradient problem. A max pooling layer follows to prevent overfitting and reduce spatial dimensionality by retaining the most prominent features within a pooling window. The operation is defined in Equation (2) [40]:

$$p_{i,j}^l = \max\left(y_{i.T+r,j}^{l-1}\right) \tag{2}$$

The model also incorporates a Batch Normalization (BN) layer to stabilize training and accelerate convergence. BN normalizes the inputs using mini-batch statistics and applies a learned scaling and bias transformation, as follows where x_i and y_i denote the input and output for the i_{th} sample, respectively, γ and β are learnable parameters, and ε is a small constant added for numerical stability [41].

$$\mu = \frac{1}{N_{batch}} \sum_{i=1}^{N} x_i \tag{3}$$

$$\sigma^2 = \frac{1}{N_{batch}} \sum_{i=1}^{N} (x_i - \mu)^2 \tag{4}$$

$$\widehat{x_i} = \frac{x_i - \mu}{\sqrt{\sigma^2 - \varepsilon}} \tag{5}$$

$$\mu y_i = \gamma x_i + \beta \tag{6}$$

Following the CNN block, a flattening layer reshapes the output into a one-dimensional array suitable for input into the BiLSTM layer, which is designed to capture sequential patterns in both forward and backward time directions. Compared to conventional RNNs, BiLSTM can retain long-term dependencies and reduce gradient degradation, making it well-suited for modeling earthquake sequences.

In the LSTM architecture, memory updates are controlled by three gates: the forget gate (f_t), which discards irrelevant information; the input gate (i_t), which updates the memory state; and the output gate (o_t), which determines the output based on the current memory state. These gates regulate information flow through the memory cell using sigmoid activations. The detailed gate computations, adapted from [32], are presented in the following equations:

$$f_t = \sigma\left(W_f . [h_{t-1}, p_t] + b_f\right) \tag{7}$$

$$i_t = \sigma(W_i . [h_{t-1}, p_t] + b_i) \tag{8}$$

$$\widehat{C_t} = tanh(W_C . [h_{t-1}, p_t] + b_C) \tag{9}$$

$$o_t = \sigma(W_o . [h_{t-1}, p_t] + b_o) \tag{10}$$

$$C_t = f_t \odot C_{t-1} + i_t \odot \widehat{C_t} \tag{11}$$

Here, h_{t-1} denotes the hidden state from the previous time step, p_i is the current input, C_t is the cell state, and σ represents the sigmoid activation function.

2.2. Methodological Framework

Figure 2 illustrates the methodological framework employed in this study. The process begins with acquiring earthquake data from the United States Geological Survey (USGS), comprising 37,316 earthquake events recorded between 1974 and 2023. The study focuses on the Indonesian region, with the spatial domain defined within the geographic extent of 95°–141°E longitude and 11°S–6°N latitude, encompassing the entire national territory.

https://doi.org/10.31436/iiumej.v26i3.3634

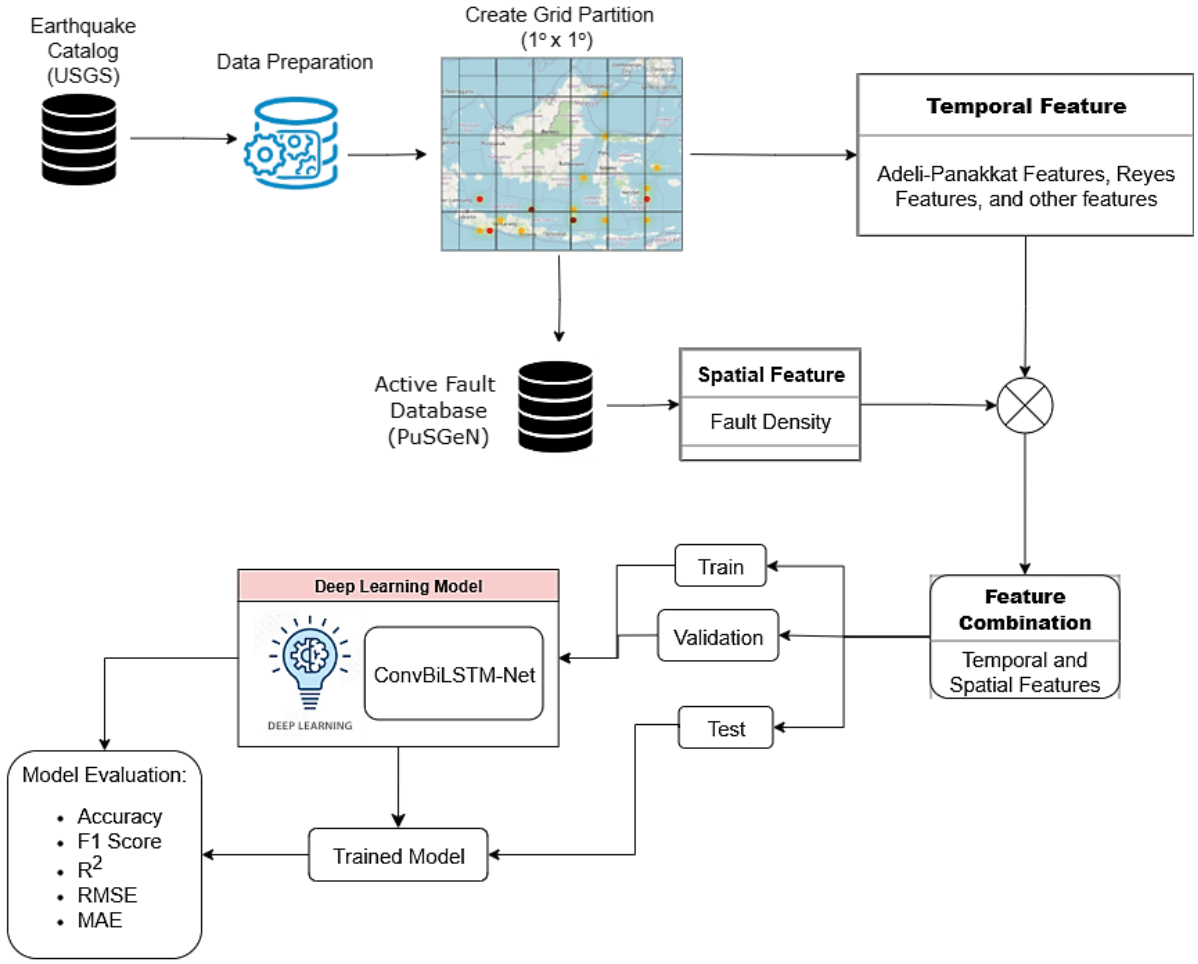

Figure 2. Methodological framework for earthquake prediction

Following data acquisition, preprocessing steps are undertaken to remove null values, duplicates, and irrelevant entries. The study area is subsequently partitioned into a grid of 1°×1° cells to facilitate spatial structuring. Each grid cell is enriched with spatial features derived from active fault data compiled in the 2017 Indonesian Earthquake Source and Hazard Map, published by the National Earthquake Study Center (PuSGeN), which includes mapped segments of active faults across the Indonesian region [42].

To characterize the spatial dimension of seismic activity, fault density (FD) is calculated using a Gaussian Kernel Density Estimation (KDE) approach. To optimize spatial representation, this study introduces a novel strategy for selecting the KDE bandwidth using the Bivariate Local Indicator of Spatial Association (LISA). This method identifies the bandwidth that yields the highest number of statistically significant local clusters (e.g., high–high, low–low), thereby ensuring spatial coherence between seismic patterns and geological fault distributions.

https://doi.org/10.31436/iiumej.v26i3.3634

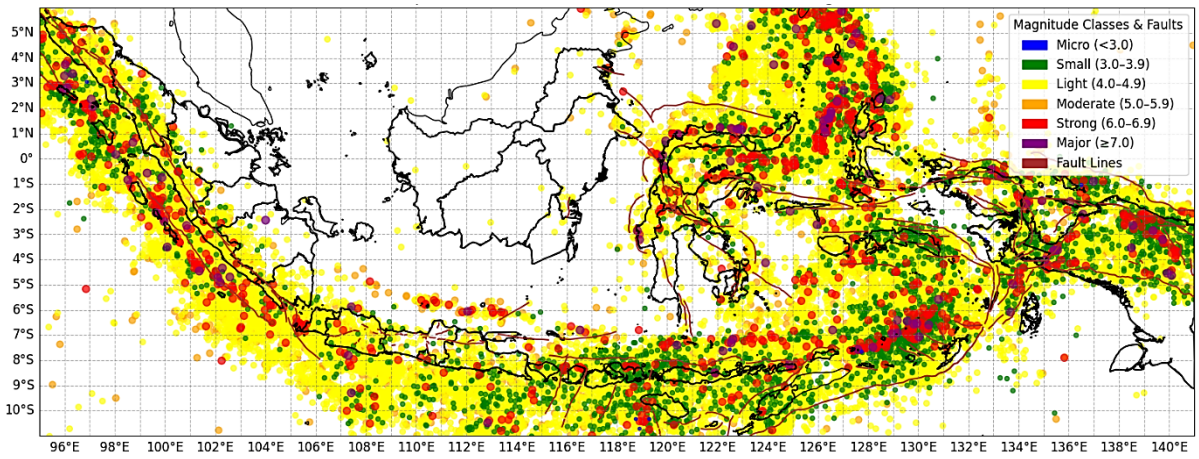

Figure 3. Spatial distribution of earthquake events in Indonesia (1974–2023), overlaid with active fault lines and classified by magnitude ranges

In parallel, the temporal dimension is captured using a comprehensive set of features derived from three established sources. First, nine statistical indicators adapted from Panakkat and Adeli [43] are employed, as presented in Table 1, including seismic productivity (a- and b-values), energy release, and inter-event times based on the Gutenberg–Richter law.

Table 1. Adeli–Panakkat Features

#	Feature	Description
1	b-value	Slope of the magnitude–log frequency plot (Gutenberg–Richter law).
2	a-value	Intercept of the Gutenberg–Richter law, representing seismic productivity.
3	H	Sum of the mean squared deviations from the regression line based on the Gutenberg–Richter law.
4	ΔM	Difference between the largest observed magnitude and the largest expected value according to the Gutenberg–Richter law.
5	T	Elapsed time between the most recent *N* earthquake events.
6	M	Average time between major seismic (characteristic) events among the last *N* events.
7	C	Coefficient of variation of the average time between characteristic events.
8	$dE^{1/2}$	The rate of the square root of the energy released.
9	M_{Mean}	Mean magnitude of the last *N* earthquake events.

In addition, seven temporal evolution metrics proposed by Reyes et al. [44] are incorporated, as summarized in Table 2. These features include successive changes in b-values and the probability of large-magnitude events. Furthermore, basic geophysical attributes, such as magnitude, depth, elapsed time, energy, and spatial coordinates, are extracted directly from the earthquake catalog, as listed in Table 3.

Table 2. Reyes Features

#	Feature	Description
1	X1	Increment of the *b*-value between events *i* and *i – 4*.
2	X2	Increment of the *b*-value between events *i – 4* and *i – 8*.
3	X3	Increment of the *b*-value between events *i – 8* and *i – 12*.
4	X4	Increment of the *b*-value between events *i – 12* and *i – 16*.
5	X5	Increment of the *b*-value between events *i – 16* and *i – 20*.
6	X6	Maximum magnitude from the events recorded in the past week (based on Omori–Utsu's law).
7	X7	Probability of recording an event with a magnitude ≥ 6.0, computed using a probability density function.

https://doi.org/10.31436/iiumej.v26i3.3634

All temporal and spatial features are combined into a unified spatiotemporal input matrix. This integrated feature set trains the proposed ConvBiLSTM-Net, a hybrid deep learning model that captures both localized spatial characteristics and long-range temporal dependencies.

The architecture begins with a one-dimensional convolutional layer (256 filters, kernel size = 3), followed by batch normalization and max pooling to extract relevant spatial patterns and suppress noise. This is followed by two stacked bidirectional long short-term memory (BiLSTM) layers (each with 256 units) that model both forward and backward temporal dynamics. Dropout layers (dropout rate = 0.3) are included after each BiLSTM layer to mitigate overfitting. Subsequently, the output is passed through a fully connected dense layer with 128 units, followed by a final dense layer with a single output neuron. This architecture trains separate models for each target variable: magnitude, depth, latitude, and longitude.

Table 3. Additional Temporal Features Extracted from the Earthquake Catalog

#	Feature	Description
1	class_mag	Classification of earthquake magnitude (e.g., small, light, moderate).
2	class_depth	Classification of earthquake depth (e.g., shallow, intermediate, deep).
3	Max magnitude expected	Maximum magnitude expected based on seismic analysis or modeling.
4	Max magnitude observed	Highest magnitude observed in the dataset.
5	Elapsed days	Total number of days elapsed since the first recorded earthquake.
6	Square root of energy	Square root of the energy released by the earthquake, often related to magnitude.
7	Timestamp	Exact time of the earthquake event (date and time).
8	Longitude	Longitude coordinate of the earthquake's epicenter.
9	Latitude	Latitude coordinate of the earthquake's epicenter.
10	Depth	Depth of the earthquake's epicenter
11	Magnitude	Magnitude of the earthquake event.

Hyperparameters are configured: learning rate = 0.001, batch size = 32, and 256 LSTM units. Early stopping based on validation loss is applied to prevent overfitting and ensure generalization. The dataset is split chronologically into 80% for training, 10% for validation, and 10% for testing. Two forecasting strategies are employed to evaluate the model's predictive performance comprehensively.

The short-term prediction task employs a sliding window approach using the most recent 30 earthquake events to forecast the subsequent (one-day-ahead) event. In contrast, the medium-term strategy involves training the model on data from 1974 to 2018 and forecasting earthquake activity for the period 2019–2023. Model performance is evaluated using both regression and classification metrics, including Accuracy, F1 Score, Coefficient of Determination (R^2), Root Mean Square Error (RMSE), and Mean Absolute Error (MAE).

2.3. Faults Density Calculation

Anselin extended the Local Moran's I statistic to develop the Local Indicators of Spatial Association (LISA) in 1995 [45]. LISA quantifies the degree of localized spatial clustering of similar values within a dataset, derived using the Local Moran Index. Unlike the global Moran's I, which measures overall spatial autocorrelation, LISA identifies local patterns of spatial dependence [46]. The Local Moran's I statistic is presented in Equation (12).

$$I_i = \frac{x_i - \bar{X}}{S_i^2} \sum_{j=1, j \neq i}^{n} w_{i,j} \left(x_j - \bar{X}\right) \quad (12)$$

LISA facilitates spatial pattern analysis at a finer scale. If the test result is statistically insignificant, no spatial autocorrelation is present. However, a significant result indicates one

https://doi.org/10.31436/iiumej.v26i3.3634

of four spatial patterns: high-high (HH), where high values are clustered together; low-low (LL), where low values cluster; high-low (HL), where low values surround high values; and low-high (LH), where high values surround low values. The sum of the individual LISA values corresponds to the global spatial association measure [47, 48].

Bivariate LISA extends this concept by correlating one variable in a given location with a different variable in neighboring areas. This approach provides a more nuanced spatial analysis, capturing localized dependencies that may not be visible in global measures. As a result, Bivariate LISA enhances the detection of spatial interactions and improves the understanding of regional variations in spatial data. The Bivariate LISA index is given in Equation (13).

$$I_B = \frac{\sum_i \ x_i(\sum_j w_{ij}(d)\, y_j\,)}{\sum_i \left(x_i\ \right)^2} \tag{13}$$

3. RESULTS AND DISCUSSION

3.1. Performance Evaluation of ConvBiLSTM-Net for Multi-Horizon Earthquake Prediction

This section empirically evaluates the proposed ConvBiLSTM-Net model for short-term and medium-term earthquake prediction. The model is tested under two feature configurations: (1) temporal features only, and (2) spatiotemporal features that integrate both spatial and temporal dimensions. The model's performance is assessed using standard evaluation metrics, including accuracy, F1 score, coefficient of determination (R^2), root mean square error (RMSE), and mean absolute error (MAE).

Table 4. Performance of the proposed ConvBiLSTM-Net model for short-term earthquake prediction.

Prediction	Feature	Accuracy	F1 Score	R^2	RMSE	MAE
Magnitude	Temporal	0.9075	0.8388	0.7367	0.0392	0.0314
	Spatiotemporal	0.9095	0.8421	0.7835	0.0371	0.0308
Depth	Temporal	0.8489	0.6509	0.8411	0.0579	0.0397
	Spatiotemporal	0.9368	0.9038	0.8595	0.0544	0.0369
Longitude	Temporal	0.7405	0.8204	0.1187	11.8287	8.3620
	Spatiotemporal	0.8773	0.8821	0.7641	5.2055	2.7096
Latitude	Temporal	0.9084	0.8405	0.2297	0.2392	0.1671
	Spatiotemporal	0.9257	0.9607	0.7531	0.1354	0.0763

Table 4 summarizes the performance of the ConvBiLSTM-Net model for short-term earthquake prediction using both temporal and spatiotemporal features. Compared to using temporal features alone, the results demonstrate that incorporating spatial features improves performance across all prediction parameters, magnitude, depth, longitude, and latitude. For magnitude prediction, the spatiotemporal model consistently outperforms the temporal-only model. Accuracy increases by 0.22%, reaching 0.9095, while the F1 score improves by 0.39%, reaching 0.8421. A notable improvement of 6.35% is observed in the coefficient of determination (R^2), indicating a stronger correlation between predicted and actual values. Meanwhile, RMSE and MAE decrease by 5.36% and 1.91%, respectively, reflecting lower prediction errors. These findings suggest incorporating spatial context enhances the model's ability to capture seismic dynamics in short-term scenarios.

https://doi.org/10.31436/iiumej.v26i3.3634

Similarly, the model exhibits substantial performance gains for depth prediction, particularly in the F1 score, which increases by 38.85%. Accuracy also improves by 10.35%, reflecting better classification performance. A moderate improvement of 2.19% is observed in R^2, accompanied by decreases in RMSE and MAE by 6.04% and 7.05%, respectively. These outcomes indicate that, although depth is primarily driven by temporal factors, integrating spatial information enhances the model's generalizability.

Moreover, incorporating spatiotemporal features significantly improves the prediction of earthquake locations, particularly in terms of latitude and longitude. For longitude prediction, the R^2 value increases dramatically by 543.72%, from 0.1187 to 0.7641, demonstrating a substantial enhancement in the model's capacity to explain variability in the data. Accuracy for longitude prediction also improves by 18.47%, reinforcing the model's effectiveness in identifying spatial patterns associated with earthquake epicenters.

Meanwhile, the RMSE decreased by 55.99%, from 11.8287 to 5.2055, and the MAE decreased by 67.61%, from 8.3620 to 2.7096. This reduction in prediction error provides strong evidence that integrating spatial features significantly enhances the model's performance in earthquake longitude prediction. For latitude, the R^2 value increased by 227.86%, from 0.2297 to 0.7531, indicating a substantial improvement in the model's ability to explain data variability. Additionally, the MAE decreased by 54.34%, from 0.1671 to 0.0763, reflecting a considerable reduction in the average prediction error. This was accompanied by a 43.39% decrease in RMSE, from 0.2392 to 0.1354. Furthermore, the accuracy increased by 1.90%, from 0.9084 to 0.9257, reinforcing the reliability of the spatiotemporal model in predicting earthquake latitude. Overall, these results further confirm the effectiveness of the proposed model in capturing the complex spatial dynamics involved in earthquake latitude prediction.

Table 5 presents the earthquake prediction results for the medium-term scenario. These findings reinforce the results presented in Table 4, indicating that the proposed model, which incorporates spatiotemporal features, enhances earthquake prediction performance in the short term. The consistent performance improvement across both temporal scenarios suggests that the ConvBiLSTM-Net model effectively captures seismic dynamics and is reliable for predicting earthquake events over medium-term horizons.

Table 5. Performance of the proposed ConvBiLSTM-Net model for medium-term earthquake prediction

Prediction	Feature	Accuracy	F1 Score	R^2	RMSE	MAE
Magnitude	Temporal	0.9031	0.8231	0.7811	0.1721	0.1381
	Spatiotemporal	0.9458	0.9082	0.9917	0.1721	0.1448
Depth	Temporal	0.9361	0.8876	0.9338	0.3899	0.0271
	Spatiotemporal	0.9388	0.8924	0.9374	0.2418	0.0185
Longitude	Temporal	0.8003	0.8891	0.0878	0.2048	0.2561
	Spatiotemporal	0.9426	0.9632	0.7589	0.2477	0.1661
Latitude	Temporal	0.8623	0.8357	0.6553	0.2584	0.1875
	Spatiotemporal	0.9314	0.9231	0.9201	0.1615	0.1005

Regarding magnitude prediction, the spatiotemporal model shows a notable performance improvement. The F1 score increased by 10.34%, from 0.8231 to 0.9082, while the coefficient of determination (R^2) rose significantly by 26.99%, from 0.7811 to 0.9917, indicating a near-perfect correlation between predicted and actual values. Although the RMSE value remained constant at 0.1721, the MAE slightly increased by 4.85%, from 0.1381 to 0.1448. Moreover, accuracy improved by 4.73%, from 0.9031 to 0.9458, further supporting the model's overall enhancement in classification performance. This overall improvement in model fit,

accompanied by a minor increase in average error, suggests that the increased complexity of medium-term seismic dynamics slightly impacts prediction accuracy.

For depth prediction, the spatiotemporal model also demonstrates meaningful improvements. The R^2 increased by 0.39%, from 0.9338 to 0.9374, while the RMSE and MAE decreased by 37.98% and 31.73%, respectively. Accuracy rose slightly by 0.29%, from 0.9361 to 0.9388, and the F1 score improved by 0.54%, from 0.8876 to 0.8924. The substantial reduction in error metrics and consistent gains in accuracy and F1 score underscore the model's ability to produce more accurate and reliable depth predictions. This improvement suggests that spatial features are crucial in capturing vertical seismic patterns over extended prediction periods.

The most significant improvement is observed in the prediction of longitude coordinates. The R^2 increased dramatically by 764.35%, from 0.0878 to 0.7589. Accuracy rose by 17.78%, from 0.8003 to 0.9426, and the F1 score increased by 8.33%, reaching 0.9632. Although RMSE slightly increased by 20.95%, from 0.2048 to 0.2477, MAE decreased substantially by 35.14%, from 0.2561 to 0.1661. This combination of enhanced accuracy and reduced average error highlights the importance of spatial components in improving the precision of east–west earthquake location predictions.

Similarly, predictions for latitude coordinates exhibit consistent performance enhancements. The R^2 increased by 40.41%, from 0.6553 to 0.9201, reflecting the model's improved capacity to capture the north–south spatial distribution of seismic events. RMSE and MAE declined sharply by 37.50% and 46.40%, respectively, to 0.1615 and 0.1005. Accuracy improved by 8.01%, from 0.8623 to 0.9314, and the F1 score rose by 10.46%, from 0.8357 to 0.9231, further supporting the model's robustness in spatial prediction tasks.

3.2. Comparative Evaluation of ConvBiLSTM-Net and Baseline Architectures for Earthquake Prediction

A comparative evaluation is conducted to benchmark the proposed ConvBiLSTM-Net model against conventional deep learning baselines, including CNN-LSTM, CNN-LSTM with Attention, and CNN-BiLSTM. All models are trained and tested using identical spatiotemporal feature inputs to ensure fairness and consistency. The evaluation focuses on four key seismic prediction targets: earthquake magnitude, depth, and epicentral coordinates (longitude and latitude), across both short-term and medium-term forecasting horizons. Model performance is assessed using a comprehensive set of predictive metrics that capture classification accuracy, regression quality, and overall prediction error.

3.2.1. Model Performance on Short-Term Earthquake Prediction

Table 6 presents the proposed ConvBiLSTM-Net model's magnitude prediction performance compared with three baseline architectures. The results indicate that the proposed model achieves the highest accuracy of 0.9095, representing a relative improvement of approximately 0.25% over the CNN-LSTM, which is the strongest baseline in terms of accuracy. Additionally, the F1 score reaches 0.8421, marking a 0.53% improvement over the average F1 score of the baseline models, and demonstrating the model's enhanced ability to balance precision and recall.

Notable improvements are also observed in the regression metrics. The proposed model achieves the lowest RMSE (0.0371) and MAE (0.0308), corresponding to a reduction in prediction error of approximately 24.45% and 9.14%, respectively, compared to the worst-performing baseline (CNN-LSTM). When compared to the best-performing baseline in terms

https://doi.org/10.31436/iiumej.v26i3.3634

of regression (CNN-BiLSTM), ConvBiLSTM-Net still demonstrates a significant reduction in error. Furthermore, the R^2 score of ConvBiLSTM-Net increases substantially to 0.7835, compared to the baseline range of 0.6231 to 0.6771. This improvement, ranging from 15.71% to 25.74%, reflects a stronger correlation between the predicted and actual magnitude values.

These results confirm the proposed architecture's superiority in capturing complex nonlinear relationships and spatiotemporal patterns in seismic data.

Table 6. Magnitude Prediction

Model	Accuracy	F1 Score	RMSE	MAE	R^2
CNN-LSTM	0.9072	0.8378	0.0491	0.0339	0.6231
CNN-LSTM with Attention	0.9071	0.8376	0.0466	0.0325	0.6578
CNN-BiLSTM	0.9071	0.8376	0.0453	0.0317	0.6771
ConvBiLSTM-Net (Proposed Model)	0.9095	0.8421	0.0371	0.0308	0.7835

Table 7 presents the performance of the proposed ConvBiLSTM-Net model in predicting earthquake depth compared to three baseline architectures. Regarding regression metrics, the proposed model achieved the lowest RMSE of 0.0544 and MAE of 0.0369, indicating a consistent improvement in prediction accuracy. Specifically, the RMSE decreased by 5.06% compared to CNN-LSTM, 3.03% compared to CNN-LSTM with Attention, and 1.81% compared to CNN-BiLSTM. Similarly, the MAE showed a significant reduction, ranging from 3.40% to 7.05% compared to the baseline models. These reductions in error metrics highlight the ConvBiLSTM-Net's advantage in minimizing deviations from actual values.

Further improvements are evident in the classification metrics. The ConvBiLSTM-Net model achieved an accuracy of 0.9368 and an F1 score of 0.9038, corresponding to relative improvements of 7.70% and 14.97%, respectively, compared to the average performance of the baseline models. Additionally, the R^2 value increased to 0.8595, representing a 1.13% improvement and indicating a stronger correlation between predicted and actual depth values.

Overall, these results reinforce the effectiveness of the ConvBiLSTM-Net model in accurately and reliably capturing spatiotemporal patterns essential for hypocenter depth estimation, outperforming conventional deep learning architectures.

Table 7. Depth Prediction

Model	Accuracy	F1 Score	RMSE	MAE	R^2
CNN-LSTM	0.8582	0.8442	0.0573	0.0382	0.8442
CNN-LSTM With Attention	0.8691	0.8511	0.0561	0.0381	0.8511
CNN-BiLSTM	0.8821	0.6631	0.0554	0.0397	0.8545
ConvBiLSTM-Net (Proposed Model)	0.9368	0.9038	0.0544	0.0369	0.8595

In line with the observed improvements in depth prediction, the ConvBiLSTM-Net model also demonstrates superior performance in predicting earthquake longitude, as shown in Table 8 The proposed model achieves the highest accuracy of 0.8773 and an F1 score of 0.8821, outperforming the average of the three baseline models by 11.61% and 17.17%, respectively. These results indicate a notable enhancement in the model's classification capability for predicting earthquake longitude.

Regarding regression metrics, ConvBiLSTM-Net also achieves the highest R^2 value of 0.7641, reflecting a stronger ability to capture variations in the longitudinal patterns of

earthquake locations. This increase in R^2 represents improvements of 16.34%, 11.94%, and 4.37% over CNN-BiLSTM, CNN-LSTM, and CNN-LSTM with Attention, respectively. While the RMSE (0.1939) and MAE (0.1327) achieved by the ConvBiLSTM-Net are comparable to those of the CNN-LSTM with Attention model, both values are higher than those produced by CNN-BiLSTM. This suggests that, although ConvBiLSTM-Net excels in correlation-based performance, it has not yet fully outperformed the baseline in minimizing absolute error for longitude estimation.

Nevertheless, integrating bidirectional temporal modeling with spatial feature extraction substantially enhances the model‘s overall predictive capability, reinforcing its effectiveness in earthquake location estimation.

Table 8. Longitude Prediction

Model	Accuracy	F1 Score	RMSE	MAE	R^2
CNN-LSTM	0.7752	0.7396	0.1684	0.1069	0.6826
CNN-LSTM With Attention	0.8258	0.8106	0.1939	0.1327	0.7321
CNN-BiLSTM	0.7572	0.7084	0.1562	0.0961	0.6568
ConvBiLSTM-Net (Proposed Model)	0.8773	0.8821	0.1939	0.1327	0.7641

Table 9 confirms that the proposed ConvBiLSTM-Net model outperforms all baseline models across the evaluated metrics for latitude prediction. The model achieves the highest accuracy of 0.9257, representing improvements of 0.64% over CNN-LSTM, 1.18% over CNN-LSTM with Attention, and 4.93% over CNN-BiLSTM. Furthermore, the F1 score reaches 0.9607, reflecting relative improvements ranging from 0.26% to 2.57% compared to the baseline models. The ConvBiLSTM-Net also yields the lowest RMSE of 0.1354, corresponding to a reduction of 14.90% from CNN-LSTM, 3.77% from CNN-LSTM with Attention, and 4.18% from CNN-BiLSTM. Similarly, the MAE decreases significantly to 0.0763, showing reductions of 35.94%, 24.60%, and 20.27% compared to CNN-LSTM, CNN-LSTM with Attention, and CNN-BiLSTM, respectively. The R^2 value increases to 0.7531, representing an improvement ranging from approximately 2.69% to 14.16%, further demonstrating the superiority of the ConvBiLSTM-Net in accurately modeling the spatial distribution of earthquake latitude coordinates.

Table 9. Latitude Prediction

Model	Accuracy	F1 Score	RMSE	MAE	R^2
CNN-LSTM	0.9198	0.9582	0.1591	0.1191	0.6597
CNN-LSTM With Attention	0.9149	0.9554	0.1407	0.1012	0.7334
CNN-BiLSTM	0.8822	0.9366	0.1413	0.0957	0.7313
ConvBiLSTM-Net (Proposed Model)	0.9257	0.9607	0.1354	0.0763	0.7531

3.2.2. Model Performance on Medium-Term Earthquake Prediction

Table 10 presents the proposed ConvBiLSTM-Net model's performance in predicting earthquake magnitude under medium-term forecasting scenarios. The model achieves an accuracy of 0.9458, reflecting an improvement of approximately 4.73% over the best-performing baseline. Likewise, the F1-score increases to 0.9082, showing a relative

https://doi.org/10.31436/iiumej.v26i3.3634

improvement of 10.30% to 10.51% compared to the baseline values (ranging from 0.8217 to 0.8231).

The model records an RMSE of 0.1721 for regression metrics, representing a prediction error reduction of approximately 7.08% to 8.87% compared to the baselines. The coefficient of determination (R^2) improves significantly to 0.8317, corresponding to an increase of 8.21% to 13.27% relative to baseline models. This elevated R^2 indicates a stronger correlation between predicted and actual magnitudes, suggesting enhanced model capability in capturing data variability.

Although the MAE value of 0.1448 is slightly higher than the most competitive baseline (0.1334), the relative increase, ranging from 1.83% to 8.57%, is marginal. This slight increase in MAE is outweighed by the substantial improvements across other key performance indicators, particularly in classification and regression accuracy. Overall, the ConvBiLSTM-Net demonstrates a robust and balanced architecture for medium-term magnitude forecasting by effectively leveraging spatiotemporal dependencies to enhance predictive accuracy and generalization.

Table 10. Magnitude Prediction

Model	Accuracy	F1 Score	RMSE	MAE	R^2
CNN-LSTM	0.9023	0.8218	0.1858	0.1391	0.7425
CNN-LSTM With Attention	0.9025	0.8217	0.1888	0.1422	0.7342
CNN-BiLSTM	0.9031	0.8231	0.1862	0.1334	0.7686
ConvBiLSTM-Net (Proposed Model)	0.9458	0.9082	0.1721	0.1448	0.8317

Table 11 presents the performance of the ConvBiLSTM-Net model in predicting earthquake focal depth under medium-term forecasting scenarios. The model achieves an accuracy of 0.9388, reflecting an improvement of approximately 2.24% over the weakest baseline (CNN-LSTM with Attention). Additionally, the F1-score improves to 0.8924, indicating a relative increase of 2.89% to 3.27% over the baseline models. This improvement highlights the model's enhanced reliability in classifying depth categories.

Regarding regression, the model achieves a mean absolute error (MAE) of 0.0185, representing a reduction of 17.04% to 29.12% compared to the baselines. This substantial decrease in MAE indicates the model's superior ability to minimize absolute prediction errors in seismic depth estimation. Furthermore, the coefficient of determination (R^2) increases to 0.9374, corresponding to an improvement of 4.91% to 9.58%. This reflects the model's enhanced capacity to capture variance in depth values and ensure a closer fit between predicted and actual outcomes.

Table 11. Depth Prediction

Model	Accuracy	F1 Score	RMSE	MAE	R^2
CNN-LSTM	0.9188	0.8653	0.3675	0.0261	0.8555
CNN-LSTM With Attention	0.9182	0.8641	0.3526	0.0244	0.8671
CNN-BiLSTM	0.9237	0.8673	0.0481	0.0223	0.8935
ConvBiLSTM-Net (Proposed Model)	0.9388	0.8924	0.2418	0.0185	0.9374

While the RMSE value of 0.2418 is considerably higher than that of the best-performing baseline model, this outcome can be attributed to the inherent sensitivity of the RMSE metric

https://doi.org/10.31436/iiumej.v26i3.3634

to outliers, particularly infrequent deep-focus seismic events. Nevertheless, the consistent improvements in classification performance and the substantial reduction in MAE suggest that the proposed ConvBiLSTM-Net model yields more reliable and practically meaningful depth estimations. Such reliability is especially critical in operational scenarios where minimizing average predictive error is more important than accounting for isolated deviations. Together, these results reinforce the robustness and generalization capability of the proposed architecture in medium-term seismic depth forecasting.

Table 12 presents the performance of the proposed ConvBiLSTM-Net model in predicting earthquake longitude under medium-term scenarios. The ConvBiLSTM-Net achieves an accuracy of 0.9426, representing an improvement ranging from approximately 1.49% to 4.18% compared to the baseline models, with the highest baseline accuracy observed in the CNN-BiLSTM (0.9288). The F1 score also increases to 0.9632, reflecting a relative improvement of approximately 0.99% to 2.67%. This enhancement demonstrates the model's stronger classification performance in distinguishing spatial categories along the longitudinal axis. Furthermore, the coefficient of determination (R^2) improves to 0.7589, representing a relative gain of approximately 6.27% to 17.56% over the baseline models. The higher R^2 value indicates the model's enhanced ability to capture spatial variance in earthquake location data. These improvements underscore the ConvBiLSTM-Net's increased capability to model and interpret spatial dependencies that characterize earthquake longitude.

Table 12. Longitude Prediction

Model	Accuracy	F1 Score	RMSE	MAE	R^2
CNN-LSTM	0.9259	0.9521	0.1684	0.1069	0.6642
CNN-LSTM With Atten	0.9048	0.9382	0.2166	0.1607	0.6454
CNN-BiLSTM	0.9288	0.9539	0.1562	0.0961	0.7142
ConvBiLSTM-Net (Proposed Model)	0.9426	0.9632	0.2477	0.1661	0.7589

However, higher absolute prediction errors accompany these gains in classification accuracy and variance explanation. The RMSE increases to 0.2477, and the MAE rises to 0.1661, corresponding to relative increases of approximately 58.58% and 72.84%, respectively, when compared to the best-performing baseline (CNN-BiLSTM), which recorded an RMSE of 0.1562 and an MAE of 0.0961. These results suggest that while the model excels at identifying spatial patterns, it may be more susceptible to larger individual prediction deviations. The elevated error values could stem from the model's sensitivity to positional outliers or broader spatial variability in longitudinal distribution. Despite this trade-off, the ConvBiLSTM-Net demonstrates strong predictive capabilities in capturing longitudinal patterns, particularly regarding accuracy, F1 score, and explained variance. While further refinement may be necessary to reduce point-specific errors, the model remains robust and well-suited for medium-term seismic spatial forecasting, especially in applications where pattern recognition and classification fidelity are prioritized.

Table 13 summarizes the medium-term latitude prediction results, indicating that the proposed ConvBiLSTM-Net establishes a new benchmark for overall performance. The model achieves an accuracy of 0.9314, representing an improvement of approximately 2.59% over the best-performing baseline model, CNN-BiLSTM (0.9078). Regarding classification quality, the F1 score rises to 0.8942, reflecting a 5.31% enhancement over the strongest baseline score of 0.8491, recorded by CNN-LSTM with Attention. The proposed model also shows a modest gain in explanatory power, with the coefficient of determination (R^2) increasing to 0.9201, equivalent to a 1.30% improvement over the CNN-BiLSTM baseline (R^2 = 0.9083). This

increase suggests a more substantial alignment between the predicted and observed spatiotemporal patterns.

A slight trade-off in absolute prediction errors accompanies these improvements. The RMSE increases to 0.1615, approximately 12.80% higher than the lowest baseline error of 0.1432 recorded by CNN-BiLSTM. Similarly, the MAE rises marginally to 0.1005, representing an increase of only 0.70% compared to the lowest baseline MAE, also achieved by CNN-BiLSTM (0.0998). Despite these modest increases in absolute error, the substantial gains in accuracy, F1 score, and R^2 underscore the ConvBiLSTM-Net model's superior ability to capture complex seismic patterns along the latitude axis. Overall, the proposed model offers the most reliable balance between classification fidelity and regression accuracy, positioning it as the most effective architecture for medium-term latitude forecasting in this study.

Table 13. Latitude Prediction

Model	Accuracy	F1 Score	RMSE	MAE	R^2
CNN-LSTM	0.8961	0.8263	0.1595	0.1209	0.9009
CNN-LSTM With Atten	0.8989	0.8491	0.2081	0.2371	0.8488
CNN-BiLSTM	0.9078	0.8172	0.1432	0.0998	0.9083
ConvBiLSTM-Net (Proposed Model)	0.9314	0.8942	0.1615	0.1005	0.9201

4. CONCLUSION

This study demonstrates that the proposed ConvBiLSTM-Net model significantly outperforms various deep learning architectures (baselines) in earthquake prediction across all key targets, namely, magnitude, depth, and epicentral coordinates (longitude and latitude), in both short-term and medium-term scenarios. In the short-term prediction scenario, ConvBiLSTM-Net consistently surpasses all baseline models. Specifically, for magnitude prediction, the model achieves a 20.05% improvement in R^2, alongside increases of 0.26% and 0.53% in accuracy and F1 score, respectively. Additionally, it reduces RMSE and MAE by 21.06% and 5.81%, reflecting enhanced precision in magnitude estimation. For depth prediction, ConvBiLSTM-Net improves accuracy by 7.70% and F1 score by 14.97%, with a modest R^2 gain of 1.13%. It also lowers RMSE and MAE by 3.32% and 4.57%, respectively, indicating overall improvement in depth prediction.

Beyond magnitude and depth, ConvBiLSTM-Net also performs strongly in epicentral coordinate prediction. For latitude prediction, the model increases R^2 by 6.35% and accuracy by 2.22%, while substantially decreasing RMSE and MAE by 7.91% and 27.56%, respectively, indicating significant spatial improvement along the north–south axis. For longitude prediction, it achieves an 11.61% gain in accuracy and a 10.66% increase in R^2. However, RMSE and MAE increase by 12.19% and 18.59%, respectively, suggesting that while the model better captures variance in longitude (as reflected by the higher R^2), it also yields higher absolute prediction errors than the baselines.

ConvBiLSTM-Net maintains superior performance across all key targets in the medium-term prediction scenario. The model achieves an R^2 improvement of 11.13% for magnitude prediction, with increased accuracy and F1 score of 4.78% and 10.46%, respectively. RMSE decreases by 7.94%, although MAE increases slightly by 4.75%, indicating better variance explanation with a minor trade-off in localized error. Regarding depth prediction, the model improves accuracy by 2.02% and F1 score by 3.10%, with a notable R^2 gain of 7.50%. It also

significantly reduces RMSE and MAE by 5.58% and 23.76%, respectively, further underscoring its ability to estimate depth precisely.

Turning to spatial prediction, the model also demonstrates notable improvements in epicentral coordinate estimation. For latitude prediction, it improves R^2 by 3.85% and accuracy by 3.38%, while significantly reducing the mean absolute error (MAE) by 34.14% and the root mean square error (RMSE) by 5.15%. These results indicate meaningful enhancements in spatial prediction accuracy along the north–south axis. For longitude prediction, ConvBiLSTM-Net achieves an R^2 improvement of 12.50%, with a 2.48% increase in accuracy and a 1.60% gain in F1 score. However, these improvements come at the cost of increased error, with RMSE and MAE rising by 37.31% and 37.01%, respectively. This suggests that although the model more effectively captures longitudinal variance, it also yields higher absolute prediction errors.

Based on these findings, ConvBiLSTM-Net demonstrates strong capabilities in modeling spatiotemporal relationships while maintaining robust and superior prediction performance across different time horizons. The model consistently enhances the accuracy of predicting all key seismic parameters, magnitude, depth, and particularly the earthquake epicenter (latitude and longitude). Notably, while absolute errors in longitude prediction increase in some instances, the model still exhibits improved pattern recognition, as indicated by higher R^2 values. By leveraging the synergy between spatial and temporal features, ConvBiLSTM-Net effectively captures complex seismic dynamics, resulting in improved generalization in both short-term and medium-term scenarios. These findings confirm its potential as a practical and adaptive solution for advancing earthquake prediction systems, particularly in enhancing epicenter localization, which is critical for early warning and disaster risk mitigation efforts.

ACKNOWLEDGEMENT

This work was supported by the Indonesian Education Scholarship (*Beasiswa Pendidikan Indonesia*, BPI), administered by the Center for Higher Education Funding and Assessment, Ministry of Higher Education, Science, and Technology of the Republic of Indonesia (PPAPT), and the Indonesia Endowment Fund for Education (*Lembaga Pengelola Dana Pendidikan*, LPDP), as acknowledged in Decree No. 02462/BPPT/BPI.06/9/2024. The authors also thank the Laboratory of Computer Systems and Networks, Department of Computer Science and Electronics, Faculty of Mathematics and Natural Sciences, Universitas Gadjah Mada, for providing technical facilities and academic support during this research.

REFERENCES

[1] Alarifi, A.S.N., Alarifi, N.S.N., Al-Humidan, S.: Earthquakes magnitude predication using artificial neural network in northern Red Sea area. J King Saud Univ Sci. 24, 301–313 (2012). https://doi.org/10.1016/j.jksus.2011.05.002.

[2] Berhich, A., Belouadha, F.-Z., Kabbaj, M.I.: An attention-based LSTM network for large earthquake prediction. Soil Dynamics and Earthquake Engineering. 165, 107663 (2023). https://doi.org/10.1016/j.soildyn.2022.107663.

[3] Shidik, G.F., Pramunendar, R.A., Kusuma, E.J., Saraswati, G.W., Winarsih, N.A.S., Rohman, M.S., Saputra, F.O., Naufal, M., Andono, P.N.: LUTanh Activation Function to Optimize BI-LSTM in Earthquake Forecasting. International Journal of Intelligent Engineering and Systems. 17, 572 – 583 (2024). https://doi.org/10.22266/ijies2024.0229.48.

[4] Maharani, E.: Infografis Kerusakan Ekonomi Akibat Gempa Besar di Dunia, https://visual.republika.co.id/berita/rrsyo1335/infografis-kerusakan-ekonomi-akibat-gempa-besar-di-dunia, last accessed 2023/10/01.

[5] UYEDA, S.: On Earthquake Prediction in Japan. Proceedings of the Japan Academy, Series B. 89, 391–400 (2013). https://doi.org/10.2183/pjab.89.391.

[6] HAYAKAWA, M., SCHEKOTOV, A., POTIRAKIS, S., EFTAXIAS, K.: Criticality features in ULF magnetic fields prior to the 2011 Tōhoku earthquake. Proceedings of the Japan Academy, Series B. 91, 25–30 (2015). https://doi.org/10.2183/pjab.91.25.

[7] Alimoradi, H., Rahimi, H., Ovaisi Moaakhar, M.: Investigation of changes in the cumulative number of magnetic anomalies before and after earthquakes using satellite data. Advances in Space Research. 75, 895–907 (2025). https://doi.org/10.1016/j.asr.2024.09.012.

[8] Wang, Q., Guo, Y., Yu, L., Li, P.: Earthquake Prediction Based on Spatio-Temporal Data Mining: An LSTM Network Approach. IEEE Trans Emerg Top Comput. 8, 148–158 (2017). https://doi.org/10.1109/TETC.2017.2699169.

[9] Kagan, Y.Y., Jackson, D.D.: Long-Term Earthquake Clustering. Geophys J Int. 104, 117–134 (1991). https://doi.org/10.1111/j.1365-246X.1991.tb02498.x.

[10] Kagan, Y.Y., Jackson, D.D.: Long-term probabilistic forecasting of earthquakes. J Geophys Res Solid Earth. 99, 13685–13700 (1994). https://doi.org/10.1029/94JB00500.

[11] Banna, Md.H. Al, Taher, K.A., Kaiser, M.S., Mahmud, M., Rahman, Md.S., Hosen, A.S.M.S., Cho, G.H.: Application of Artificial Intelligence in Predicting Earthquakes: State-of-the-Art and Future Challenges. IEEE Access. 8, 192880–192923 (2020). https://doi.org/10.1109/ACCESS.2020.3029859.

[12] Mojtahedi, F.F., Yousefpour, N., Chow, S.H., Cassidy, M.: Deep Learning for Time Series Forecasting: Review and Applications in Geotechnics and Geosciences. Archives of Computational Methods in Engineering. (2025). https://doi.org/10.1007/s11831-025-10244-5.

[13] Majumder, R.Q.: Machine Learning for Predictive Analytics: Trends and Future Directions. SSRN Electronic Journal. (2025). https://doi.org/10.2139/ssrn.5267273.

[14] Jamarani, A., Haddadi, S., Sarvizadeh, R., Haghi Kashani, M., Akbari, M., Moradi, S.: Big data and predictive analytics: A systematic review of applications. Artif Intell Rev. 57, 176 (2024). https://doi.org/10.1007/s10462-024-10811-5.

[15] Huang, C.-J., Kuo, P.-H.: A Short-Term Wind Speed Forecasting Model by Using Artificial Neural Networks with Stochastic Optimization for Renewable Energy Systems. Energies (Basel). 11, 2777 (2018). https://doi.org/10.3390/en11102777.

[16] Peng, L., Wang, L., Ai, X.-Y., Zeng, Y.-R.: Forecasting Tourist Arrivals via Random Forest and Long Short-term Memory. Cognit Comput. 13, 125–138 (2021). https://doi.org/10.1007/s12559-020-09747-z.

[17] Li, X., Wu, P.: Stock Price Prediction Incorporating Market Style Clustering. Cognit Comput. 14, 149–166 (2022). https://doi.org/10.1007/s12559-021-09820-1.

[18] Wang, X., Nguyen, K., Nguyen, B.P.: Churn Prediction using Ensemble Learning. In: Proceedings of the 4th International Conference on Machine Learning and Soft Computing. pp. 56–60. ACM, New York, NY, USA (2020). https://doi.org/10.1145/3380688.3380710.

[19] Asim, K.M., Martínez-Álvarez, F., Basit, A., Iqbal, T.: Earthquake magnitude prediction in Hindukush region using machine learning techniques. Natural Hazards. 85, 471–486 (2017). https://doi.org/10.1007/s11069-016-2579-3.

[20] Asim, K.M., Idris, A., Iqbal, T., Martínez-Álvarez, F.: Earthquake prediction model using support vector regressor and hybrid neural networks. PLoS One. 13, e0199004 (2018). https://doi.org/10.1371/journal.pone.0199004.

[21] Yaghmaei-Sabegh, S., Tsang, H.-H.: A new site classification approach based on neural networks. Soil Dynamics and Earthquake Engineering. 31, 974–981 (2011). https://doi.org/10.1016/j.soildyn.2011.03.004.

[22] Asim, K.M., Moustafa, S.SR., Niaz, I.A., Elawadi, E.A., Iqbal, T., Martínez-Álvarez, F.: Seismicity analysis and machine learning models for short-term low magnitude seismic activity

predictions in Cyprus. Soil Dynamics and Earthquake Engineering. 130, 105932 (2020). https://doi.org/10.1016/j.soildyn.2019.105932.

[23] Jain, R., Nayyar, A., Arora, S., Gupta, A.: A comprehensive analysis and prediction of earthquake magnitude based on position and depth parameters using machine and deep learning models. Multimed Tools Appl. 80, 28419–28438 (2021). https://doi.org/10.1007/s11042-021-11001-z.

[24] Gonzalez, J., Yu, W., Telesca, L.: Gated Recurrent Units Based Recurrent Neural Network for Forecasting the Characteristics of the Next Earthquake. Cybern Syst. 53, 209–222 (2022). https://doi.org/10.1080/01969722.2021.1981637.

[25] Kavianpour, P., Kavianpour, M., Ramezani, A.: Deep Multi-scale Dilated Convolution Neural Network with Attention Mechanism: A Novel Method for Earthquake Magnitude Classification. In: 2022 8th Iranian Conference on Signal Processing and Intelligent Systems (ICSPIS). pp. 1–6 (2022). https://doi.org/10.1109/ICSPIS56952.2022.10043978.

[26] Cai, Y., Shyu, M.-L., Tu, Y.-X., Teng, Y.-T., Hu, X.-X.: Anomaly detection of earthquake precursor data using long short-term memory networks. Applied Geophysics. 16, 257–266 (2019). https://doi.org/10.1007/s11770-019-0774-1.

[27] Fabregas, A.C., Arellano, P.B. V., Pinili, A.N.D.: Long-Short Term Memory (LSTM) Networks with Time Series and Spatio-Temporal Approaches Applied in Forecasting Earthquakes in the Philippines. In: Proceedings of the 4th International Conference on Natural Language Processing and Information Retrieval. pp. 188–193. ACM, New York, NY, USA (2020). https://doi.org/10.1145/3443279.3443288.

[28] Berhich, A., Belouadha, F.-Z., Kabbaj, M.I.: An attention-based LSTM network for large earthquake prediction. Soil Dynamics and Earthquake Engineering. 165, 107663 (2023). https://doi.org/10.1016/j.soildyn.2022.107663.

[29] Kail, R., Burnaev, E., Zaytsev, A.: Recurrent Convolutional Neural Networks Help to Predict Location of Earthquakes. IEEE Geoscience and Remote Sensing Letters. 19, 1–5 (2022). https://doi.org/10.1109/LGRS.2021.3107998.

[30] Bhandarkar, T., K, V., Satish, N., Sridhar, S., Sivakumar, R., Ghosh, S.: Earthquake trend prediction using long short-term memory RNN. International Journal of Electrical and Computer Engineering (IJECE). 9, 1304 (2019). https://doi.org/10.11591/ijece.v9i2.pp1304-1312.

[31] Kavianpour, P., Kavianpour, M., Jahani, E., Ramezani, A.: A CNN-BiLSTM model with attention mechanism for earthquake prediction. J Supercomput. 80, 2913–2913 (2024). https://doi.org/10.1007/s11227-023-05497-5.

[32] Kavianpour, P., Kavianpour, M., Jahani, E., Ramezani, A.: Earthquake Magnitude Prediction using Spatia-Temporal Features Learning Based on Hybrid CNN-BiLSTM Model. In: Proceedings - 2021 7th International Conference on Signal Processing and Intelligent Systems, ICSPIS 2021. Institute of Electrical and Electronics Engineers Inc. (2021). https://doi.org/10.1109/ICSPIS54653.2021.9729358.

[33] Geng, Y., Su, L., Jia, Y., Han, C.: Seismic Events Prediction Using Deep Temporal Convolution Networks. Journal of Electrical and Computer Engineering. 2019, 1–14 (2019). https://doi.org/10.1155/2019/7343784.

[34] Yousefzadeh, M., Hosseini, S.A., Farnaghi, M.: Spatiotemporally explicit earthquake prediction using deep neural network. Soil Dynamics and Earthquake Engineering. 144, 106663 (2021). https://doi.org/10.1016/j.soildyn.2021.106663.

[35] Hetényi, G., Epard, J.-L., Colavitti, L., Hirzel, A.H., Kiss, D., Petri, B., Scarponi, M., Schmalholz, S.M., Subedi, S.: Spatial relation of surface faults and crustal seismicity: a first comparison in the region of Switzerland. Acta Geodaetica et Geophysica. 53, 439–461 (2018). https://doi.org/10.1007/s40328-018-0229-9.

[36] Matsuda, T.: Estimation of Future Destructive Earthquakes from Active Faults on Land in Japan. Journal of Physics of the Earth. 25, S251–S260 (1977). https://doi.org/10.4294/jpe1952.25.Supplement_S251.

[37] Matsuda, T.: Active Faults and Damaging Earthquakes in Japan-Macroseismic Zoning and Precaution Fault Zones. (2013). https://doi.org/10.1029/ME004p0279.

[38] Sharma, A., Ahuja, A., Devi, S., Pasari, S.: Use of Spatio-temporal Features for Earthquake Forecasting of imbalanced Data. In: 2022 International Conference on Intelligent Innovations in Engineering and Technology (ICIIET). pp. 178–182. IEEE (2022). https://doi.org/10.1109/ICIIET55458.2022.9967687.

[39] Song, W., Wang, C., Chen, W., Zhang, X., Li, H., Li, J.: Unlocking the spatial heterogeneous relationship between Per Capita GDP and nearby air quality using bivariate local indicator of spatial association. Resour Conserv Recycl. 160, 104880 (2020). https://doi.org/10.1016/j.resconrec.2020.104880.

[40] Phan, H., Andreotti, F., Cooray, N., Chen, O.Y., De Vos, M.: DNN Filter Bank Improves 1-Max Pooling CNN for Single-Channel EEG Automatic Sleep Stage Classification. In: 2018 40th Annual International Conference of the IEEE Engineering in Medicine and Biology Society (EMBC). pp. 453–456. IEEE (2018). https://doi.org/10.1109/EMBC.2018.8512286.

[41] Qiao, M., Yan, S., Tang, X., Xu, C.: Deep Convolutional and LSTM Recurrent Neural Networks for Rolling Bearing Fault Diagnosis Under Strong Noises and Variable Loads. IEEE Access. 8, 66257–66269 (2020). https://doi.org/10.1109/ACCESS.2020.2985617.

[42] PuSGeN: Peta Sumber Daya dan Bahaya Gempa Indonesia Tahun 2017. Puslitbang PUPR, Indonesia (2017).

[43] Adeli, H., Panakkat, A.: A probabilistic neural network for earthquake magnitude prediction. Neural Networks. 22, 1018–1024 (2009). https://doi.org/10.1016/j.neunet.2009.05.003.

[44] Reyes, J., Morales-Esteban, A., Martínez-Álvarez, F.: Neural networks to predict earthquakes in Chile. Appl Soft Comput. 13, 1314–1328 (2013). https://doi.org/10.1016/j.asoc.2012.10.014.

[45] Anselin, L.: Local Indicators of Spatial Association, LISA. Geogr Anal. 27, 93–115 (1995). https://doi.org/10.1111/j.1538-4632.1995.tb00338.x.

[46] Lee, J., Wong, D.W.S.: Statistical Analysis with ArcView GIS. John Wiley & Sons, New York (2001).

[47] Mathur, M.: Spatial autocorrelation analysis in plant population: An overview. Journal of Applied and Natural Science. 7, 501–513 (2015). https://doi.org/10.31018/jans.v7i1.639.

[48] Gao, Y., Cheng, J., Meng, H., Liu, Y.: Measuring spatio-temporal autocorrelation in time series data of collective human mobility. Geo-spatial Information Science. 22, 166–173 (2019). https://doi.org/10.1080/10095020.2019.1643609.